Article

Seasonal and annual variations in atmospheric Hg and Pb isotopes in Xi'an, China

Hongmei Xu, Jeroen E. Sonke, Benjamin Guinot, Xuewu Fu, Ruoyu Sun, Aurelie Lanzanova, Frederic Candaudap, Zhenxing Shen, and Jun-ji Cao

Environ. Sci. Technol., **Just Accepted Manuscript** • DOI: 10.1021/acs.est.6b06145 • Publication Date (Web): 02 Mar 2017

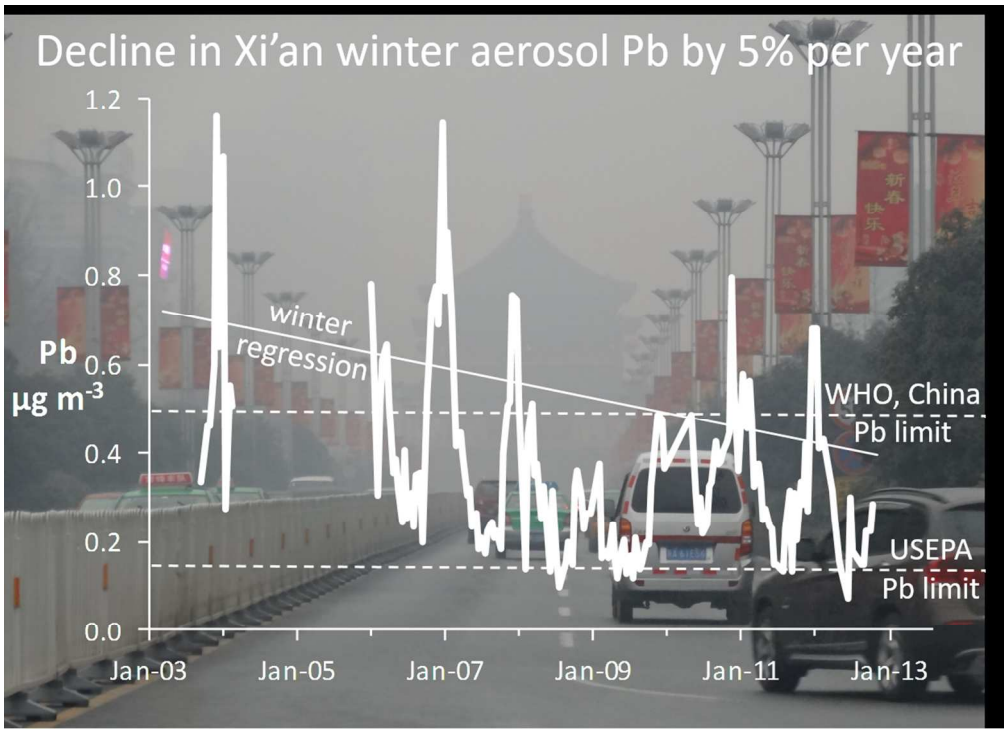

TOC Figure

209x151mm (150 x 150 DPI)

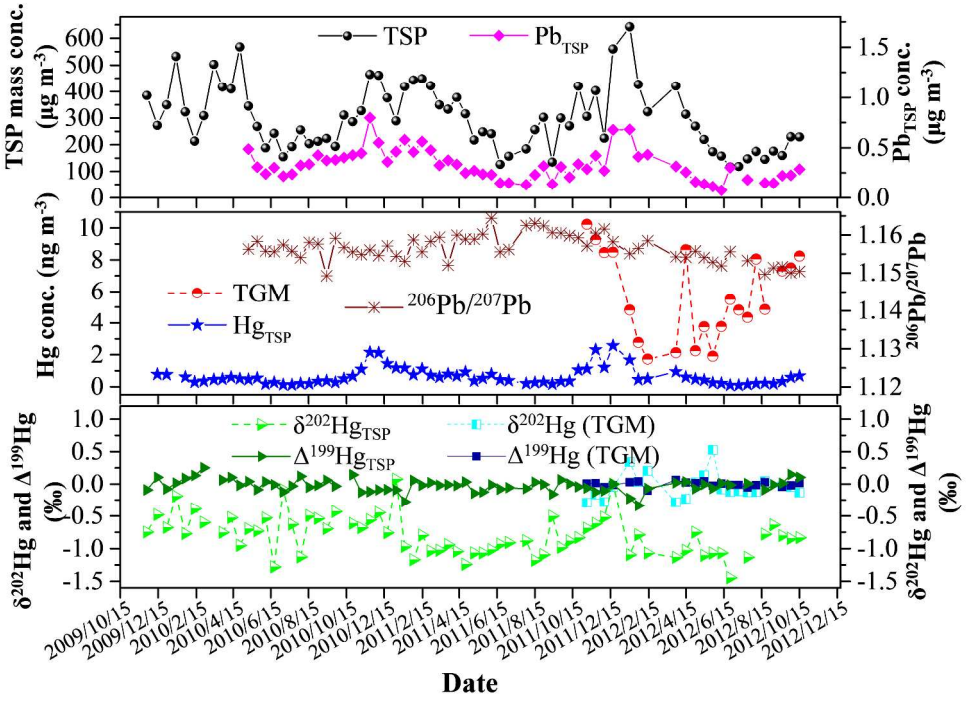

Figure 1. Temporal variations of TSP and PbTSP concentrations (conc., upper panel), particulate and total gaseous Hg concentrations, and 206Pb/207Pb ratio (middle panel), and particulate and total gaseous Hg isotopes (δ202Hg, Δ199Hg) during the sampling period in Xi'an.

1044x771mm (144 x 144 DPI)

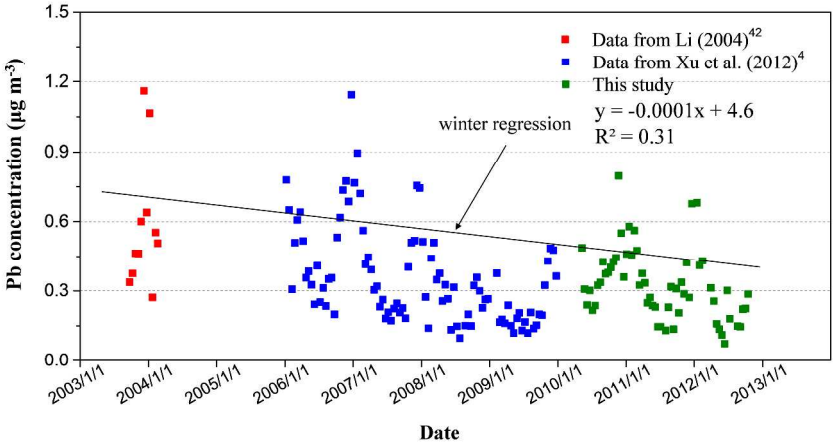

Figure 2. Summary of published aerosol Pb (μg m-3) observations in Xi'an. Data4, 42 were made on PM2.5, whereas this study measured TSP. The ensemble of observations points at a steady decline in winter time aerosol Pb of about 5% per year over the 2003-2012 period (r2 = 0.31).

1381x677mm (144 x 144 DPI)

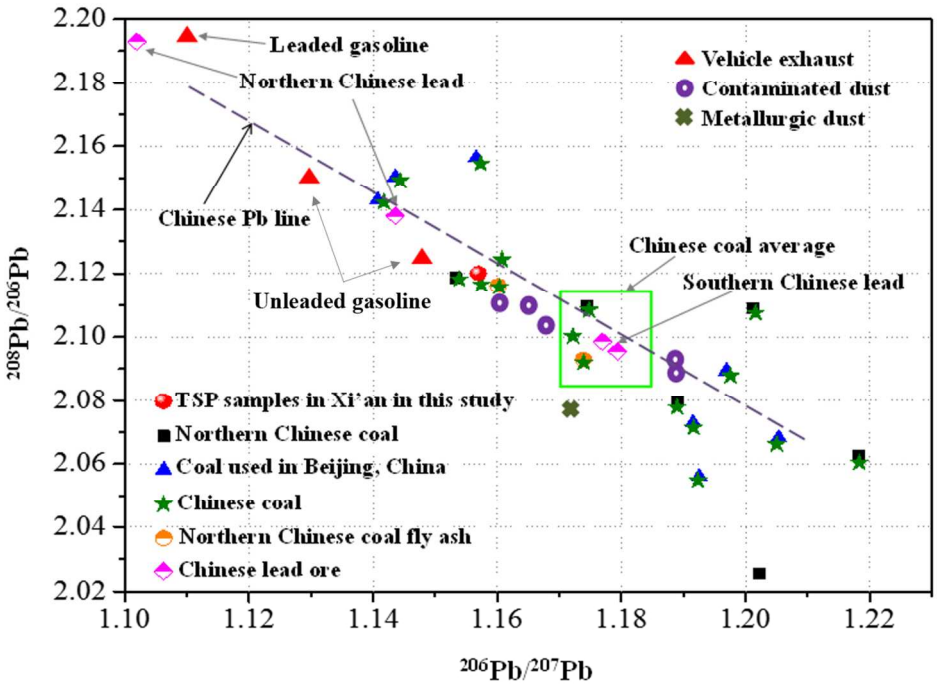

Figure 3. Scatter plots of isotopic ratios of Pb (208Pb/206Pb and 206Pb/207Pb) for TSP samples collected from Nov. 2009 to Oct. 2012 in Xi'an and for potential Pb pollution sources47-50, 62-66 in China. (the Chinese Pb line was drawn using the data for major lead mines in China48).

360x263mm (96 x 96 DPI)

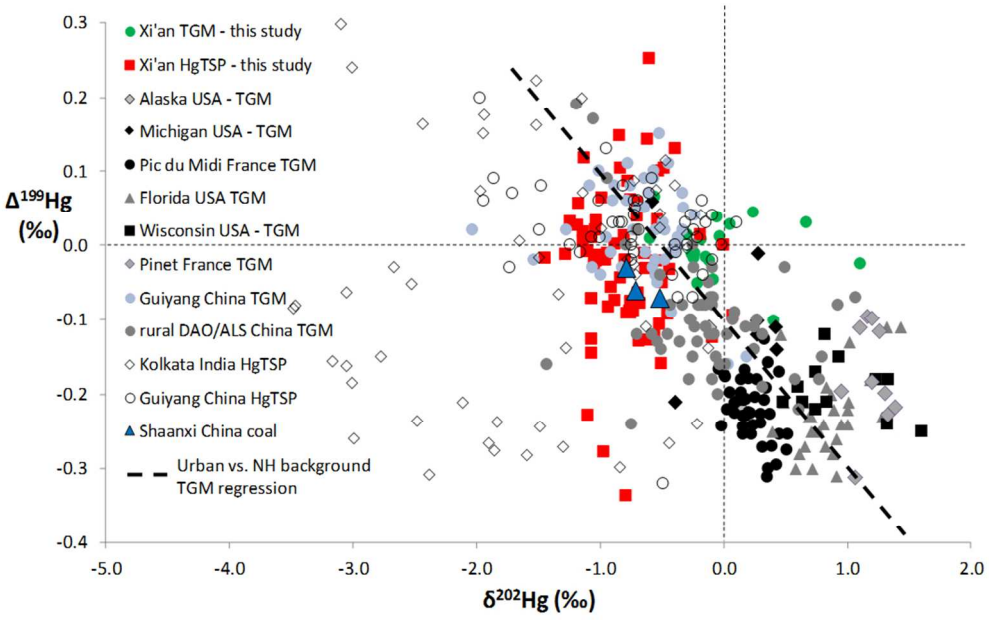

Figure 4. δ202Hg and Δ199Hg signatures of TGM (●) and HgTSP (■) in Xi'an and at other locations (diverse filled symbols). The dark black striped line (Δ199Hg = -0.2×δ202Hg - 0.1) represent the mixing line between the Northern Hemisphere (NH) background TGM and recent industrial TGM emissions discussed in the text. Also shown are coal samples (▲) from three Shaanxi coal mines that supply Xi'an domestic and industrial coal use18, 23, 39, 51, 52, 54-57.

303x189mm (90 x 90 DPI)

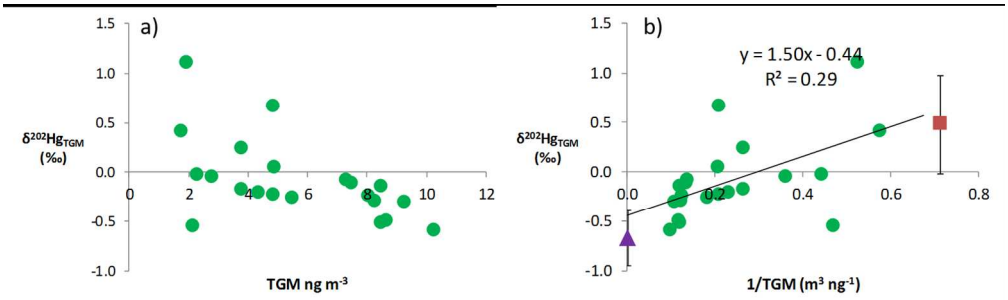

Figure 5. a): δ202HgTGM (‰) as a function of TGM concentration (ng m-3) in Xi'an. b): linearized (1/THg) binary isotope mixing diagram between the Northern Hemispheric background TGM (■, 1.4 ng m-3; δ202HgTGM of 0.47 ± 0.45‰, 2σ) and local Xi'an urban-industrial TGM emissions, represented by Shaanxi coal (▲, δ202HgShaanxi coal of -0.67 ± 0.28‰, 2σ, and assuming no shift in δ202Hg between coal Hg and emitted TGM).

266x81mm (150 x 150 DPI)

Seasonal and annual variations in atmospheric Hg and Pb isotopes in Xi'an, China

Hongmei Xu[1,2,4], Jeroen E. Sonke[3*], Benjamin Guinot[4], Xuewu Fu[6,3], Ruoyu Sun[5,3], Aurélie Lanzanova[3], Frédéric Candaudap[3], Zhenxing Shen[1], Junji Cao[2*]

[1]Department of Environmental Science and Engineering, Xi'an Jiaotong University, Xi'an, China

[2]Key Lab of Aerosol Chemistry & Physics, SKLLQG, Institute of Earth Environment, Chinese Academy of Sciences, Xi'an, China

[3]Observatoire Midi-Pyrénées, Laboratoire Géosciences Environnement Toulouse, CNRS/IRD/Université de Toulouse, France

[4]Laboratoire d'Aérologie, Université de Toulouse, CNRS, UPS, France

[5]Institute of Surface-Earth System Science, Tianjin University, Tianjin 300072, China

[6]State Key Laboratory of Environmental Geochemistry, Institute of Geochemistry, Chinese Academy of Sciences, Guiyang, 550081, China

*Corresponding authors: Jeroen E. Sonke: jeroen.sonke@get.omp.eu, 14 avenue Edouard Belin, 31400 Toulouse, France, t.:+33(0)561332606, f.:+33(0)561332560; Junji Cao: cao@loess.llqg.ac.cn, 97 Yanxiang Road, Xi'an, 710061, Shaanxi, China, t.: +86(29)62336205, f.: +86(29)62336234.

Abstract

We present a 3-year time series of lead (Pb) and mercury (Hg) concentrations and isotope signatures in total suspended particulate (TSP) matter and as total gaseous Hg (TGM) in Xi'an, Northwestern China. Mean concentrations of TSP (299 ± 120 μg m^{-3}), Pb_{TSP} (0.33 ± 0.15 μg m^{-3}) and Hg_{TSP} (0.64 ± 0.54 ng m^{-3}), and TGM (5.7 ± 2.7 ng m^{-3}) were elevated. We find that atmospheric Pb levels in Xi'an have decreased by 4.6% per year since 2003, yet remain elevated relative to air quality guidelines and therefore a major health concern. $\delta^{202}Hg_{TSP}$ and $\Delta^{199}Hg_{TSP}$ averaged -0.80 ± 0.30 ‰ (1σ) and -0.02 ± 0.10 ‰ (1σ) and $\delta^{202}Hg_{TGM}$ and $\Delta^{199}Hg_{TGM}$ averaged -0.08 ± 0.41 ‰ (1σ) and 0.00 ± 0.04 ‰ (1σ). Relative to raw coal from Shaanxi and surrounding provinces, $\delta^{202}Hg_{TSP}$ is enriched in the light Hg isotopes, while $\delta^{202}Hg_{TGM}$ is enriched in the heavy isotopes. TSP and TGM $\Delta^{199}Hg$ signatures are indistinguishable from raw coal, indicating little photochemical mass independent fractionation of atmospheric Hg in the near-field urban-industrial environment. $\delta^{202}Hg_{TGM}$ correlates significantly with TGM levels (r^2 = 0.3, p<0.01) and likely reflects binary mixing of local industrial TGM emissions with global background TGM.

Keywords: heavy metals; lead and mercury isotopes; atmospheric emission; China

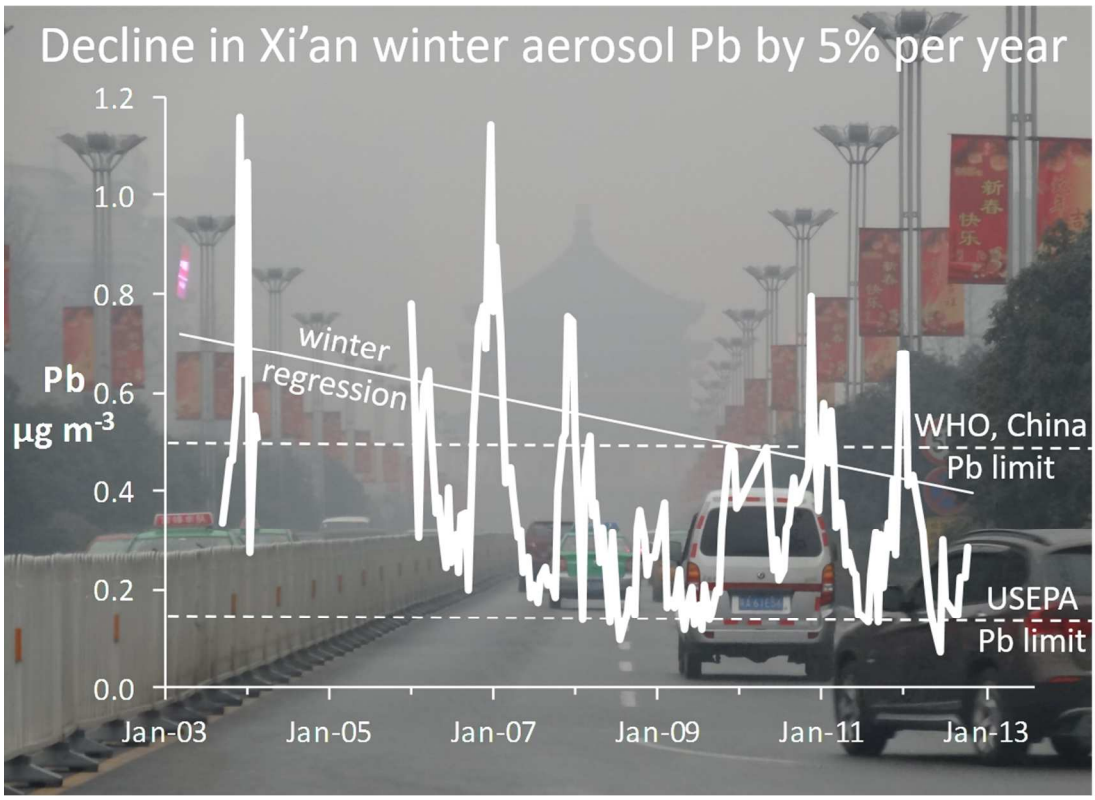

TOC Figure. Photo by Hongmei Xu in Xi'an landmark-Bell Tower, China in February 2013.

Introduction

An important component of atmospheric pollution in China is associated with heavy metals, e.g. lead (Pb) and mercury (Hg). Both Pb and Hg are neuro-developmental toxins at low exposure doses, though exposure routes differ substantially[1,2]. Together with drinking water and food, inhalation of atmospheric particles is an important exposure pathway for Pb[1]. Leaded gasoline was phased-out in the 1990's in China (2000 in Xi'an). A recent review on Pb pollution in China suggests that Pb emission from the energy and industrial sectors, i.e. coal combustion, is presently of the same order of magnitude as leaded gasoline emissions in China[3]. $^{206}Pb/^{207}Pb$ and $^{208}Pb/^{206}Pb$ ratios in Xi'an, China, winter and summer between 2007 and 2009 confirmed the impact of coal combustion on $PM_{2.5}$ Pb concentrations in winter and indicated a dominant contribution of motor vehicular emission to $PM_{2.5}$ Pb in summer in Xi'an[4]. The relatively dramatic rise in coal combustion Pb emissions has been caused by the growing energy demand, the phasing out of leaded gasoline and the slow implementation of emission control technologies[3,4].

Recent increase in child blood lead levels (BLL) in Shanghai has been found to correlate with atmospheric Pb levels and regional coal consumption[5]. Before the ban on leaded gasoline in the United States, typical urban US atmospheric Pb levels were around μg m^{-3} and child BLLs around 15 μg dL^{-1} [6]. Mean atmospheric Pb levels in China today range from ~0.05 μg m^{-3} in rural areas to ~0.5 μg m^{-3} in more industrialized regions[7] and urban children's BLLs range from 5.0-9.0 μg dL^{-1}, with a mean of 8.8 μg dL^{-1} [8, 9].

Seasonal and event-based atmospheric Pb regularly reaches 1 μg m^{-3}. The geometric mean of BBL in 1662 children aged 0-6 years in Xi'an was 5.8 μg dL^{-1} in 2010-2011[10]. China's Ambient Air Quality Standards (AAQS, GB 3095-2012)[11] (0.5 μg m^{-3}), WHO (0.5 μg m^{-3}) and US EPA (0.15 μg m^{-3}) atmospheric Pb guidelines, and WHO (10 μg dL^{-1}) and US CDC (5 μg dL^{-1}) child BLL guidelines are close to or exceed observed mean atmospheric Pb and child BLL in urban China. US CDC emphasized that "No safe BLL in children has been identified". Lead exposure to urban Chinese children is therefore a major health concern.

Hg emissions in China are dominated by the energy and industrial sectors. Hg emissions to the atmosphere from anthropogenic sources have been estimated to be in the range of 500-700 tons per year in China, reaching a global share of 25%-30% of total anthropogenic Hg emissions[12]. Anthropogenic Hg emissions are in the forms Hg_{TSP}, gaseous oxidized Hg (GOM) and gaseous elemental Hg (GEM). Following deposition inorganic Hg can be transformed in aquatic ecosystems to the bio-accumulating methyl-Hg form[13]. Consequently, humans are mainly exposed to methyl-Hg by consuming fresh water and marine fish. In China, the potential exposure to methyl-Hg via consumption of contaminated rice is a topic of debate[14, 15]. A substantial fraction of emitted Hg_{TSP} and GOM in China is deposited locally[16]. Because of the long atmospheric residence time of GEM (4-6 months)[17, 18], much of the emitted Hg, however, is transported into the global environment and deposits to remote ecosystems. Tracing and

evaluating the impact of Hg emissions across the globe is a challenging but necessary requirement to curb future Hg emissions. Potential chemical tracers are GEM/CO ratios or Hg stable isotope ratios[19].

Over a decade of research on the natural variations in Hg stable isotope abundance ratios have shown large variations across biogeochemical reservoirs. These variations result from the gradual separation of heavy/light or even/odd Hg isotopes during the numerous physico- and photo-chemical processes that shuttle Hg across the Earth's surface. As a result, a Hg isotope measurement gives rise to multiple isotope signatures (δ^{202}Hg, Δ^{199}Hg, etc.) that may characterize its source, or code for the transformations that Hg has undergone in the past. Recent studies of Hg isotope signatures in Chinese coal reveal substantial variation in δ^{202}Hg and Δ^{199}Hg[20-23]. In this study, we document 3 years (2009-2012) of bi-weekly variations in TSP, atmospheric particulate Pb and Hg, total gaseous Hg concentrations, and associated Pb and Hg isotope signatures in urban Xi'an (China). The main objective was to better understand the sources and evolution of atmospheric Pb and Hg in Xi'an. We also aimed to document the Pb and Hg isotope signatures at the source of Asian pollution outflow to the regional and global atmosphere.

Materials and Methods

The sampling site (E 108.887°, N 34.229°) was located in downtown Xi'an (Shaanxi, China) on a rooftop of the Institute of Earth Environment, Chinese Academy of Sciences

(Figure S1), 10 m above ground level. TSP was sampled from Nov. 2009 to Oct. 2012 at a nominal flow rate of 5 L min^{-1} on pre-fired (450^{o}C, 2 h), pre-weighed 47mm quartz fiber filters (QF-5, Millipore AQFA04700) in a Teflon filter pack. Total gaseous Hg (TGM = GEM+GOM) was sampled on iodated carbon traps (Brooks Rand) in 2012, preceded by a 47mm quartz fiber filter (QF-0.3), at a nominal flow rate of 0.3 L min^{-1} following published methods[24]. Both TSP on QF-5 and QF-0.3 filters and TGM sampling integrated 2 week periods. Sampled air volumes were measured with gas volume meters (JHC, France).

Accumulated TSP mass was weighed on a microbalance (mean 0.03 g of TSP per QF-5 filter) and expressed in μg m^{-3} relative to the sampled volume. Particulate Hg (Hg_{TSP}) was measured by combusting whole QF-0.3 filters in a Milestone DMA-80 Hg analyzer at the Observatoire Midi-Pyrenees (OMP; limit of detection 0.1 ng Hg; QF-0.3 blanks 0.2 ng Hg (n=5); mean QF-0.3 Hg content 11.5 ng Hg; long-term reproducibility on NIST-2632d coal containing 92.8 ± 3.3 ng g^{-1} Hg was 97.0 ± 7.9 ng g^{-1}, 1σ, n=16).

Total carbon (TC_{TSP}) was determined on 0.5 cm^2 punch-outs of the QF-5 filters, using a carbon analyzer at OMP (Ströhlein Coulomat 702C). The quartz filter samples were first subjected to a thermal pretreatment step (kept at 60°C for at least 15 mins) in order to remove the volatile organic compounds (VOCs). Subsequently the filters were combusted at 1200°C and detected as CO_2 in the carbon analyzer.

TSP on QF-5 filters was extracted in bi-distilled HNO_3 (3.75 mL) and HCl (1.25 mL) in 50 mm closed Teflon vessels on a hot plate at 120^{o}C for 6h. Small aliquots were diluted to a final concentration of 0.32N HNO_3 for trace element analysis by quadrupole ICPMS (Agilent 7500) at OMP following published protocols (using In and Re internal standards, and SLRS-5 for quality control)[25]. A second aliquot was diluted to 1 ng g^{-1} Pb concentration in 0.32N HNO_3 for Pb isotope ratio analysis by sector field ICPMS (Thermo-Scientific Element-XR) at OMP[26], using NIST 981 as a bracketing standard. Long-term reproducibility on NIST 981 was 0.09% and 0.07% (1σ, n=18) on the $^{208}Pb/^{206}Pb$ and $^{206}Pb/^{207}Pb$ ratios at 1 ng g^{-1} Pb. Certified reference material BCR-482 (lichen) was processed and analyzed identically. Measured $^{208}Pb/^{206}Pb$ and $^{206}Pb/^{207}Pb$ ratios for BCR-482 of 2.129 ± 0.001 and 1.131 ± 0.001 are identical within errors to purified BCR-482 Pb analyzed by MC-ICPMS, $^{208}Pb/^{206}Pb$ and $^{206}Pb/^{207}Pb$ of 2.1288 ± 0.0003 and 1.1310 ± 0.0001[27]. The remaining QF-5 extract solutions were diluted to 20 vol%, 3:1 HNO_3:HCl for Hg stable isotope analysis.

Iodated carbon, also used to collect TGM, was removed from the glass trap tubes and combusted in a dual-stage tube furnace to liberate sorbed TGM as Hg^0 following published protocols[24]. The liberated Hg^0 was trapped in a 40 vol% 3:1 HNO_3:HCl oxidizing solution. All solution traps were diluted to 20 vol% 3:1 HNO_3:HCl solutions and analyzed for Hg isotope ratios by cold vapor-multi-collector ICPMS (Thermo-Finnigan Neptune) at OMP following published protocols[28]. The Hg isotopic

composition is reported in delta notation (δ) in units of per mil (‰) referenced to the bracketed NIST 3133 Hg standard:

$$\delta^{xxx}Hg = \left(\frac{\frac{xxx}{198}Hg_{sample}}{\frac{xxx}{198}Hg_{NIST\ 3133}} - 1 \right)$$

where '*xxx*' refers to measured isotope masses 199, 200, 201, 202. Mass independent fractionation (MIF) signatures are reported in "capital delta (Δ)" notation (‰), defined as the difference between the measured δ^{199}Hg, δ^{200}Hg, δ^{201}Hg and those predicted from δ^{202}Hg using the kinetic Mass dependent fractionation (MDF) law:

$$\Delta^{xxx}\mathrm{Hg} = \delta^{xxx}\mathrm{Hg} - \beta_{xxx} \times \delta^{202}\mathrm{Hg}$$

where the mass-dependent scaling factor β_{xxx} is 0.252 for ^{199}Hg, 0.502 for ^{200}Hg and 0.752 for ^{201}Hg. Repeat analysis of reference materials UM-Almaden yielded δ^{202}Hg of -0.48 ± 0.13‰ (2σ, n=22) and Δ^{199}Hg of -0.01 ± 0.12‰ (2σ, n=22), and BCR-482 lichen yielded δ^{202}Hg of -1.51 ± 0.16‰ (2σ, n=5) and Δ^{199}Hg of -0.61 ± 0.11‰ (2σ, n=5), in agreement with published values[29, 30]. Sample analysis uncertainty was taken as the larger of 2σ values on sample analysis replicates or our BCR-482.

Statistical analysis of the observations first assessed whether data was distributed normally, followed by appropriate parametric (mean, standard deviation, t-test) or non-parametric (median, inter-quartiles, Mann-Whitney) descriptors and testing. Meteorological factors including temperature, dew-point, relative humidity (RH), precipitation, sea level pressure, visibility, and wind speed (the average of daily value)

were obtained from Shaanxi Meteorological Bureau (Xi'an, China) and Xi'an Statistical Yearbook (2010-2013)[31] (Table S1).

Results and Discussion

TSP, TC, Pb and Hg concentrations The time series of TSP mass concentration observed during the entire sampling period is shown in Figure 1. The average TSP concentrations were 307 ± 114 μg m^{-3} (ranging from 155-568 μg m^{-3}) in Nov. 2009-Oct. 2010, 316 ± 104 μg m^{-3} (ranging from 126-465 μg m^{-3}) in Nov. 2010-Oct. 2011 and 270 ± 143 μg m^{-3} (ranging from 117-642 μg m^{-3}) in Nov. 2011-Oct. 2012, respectively, with the average value of 299 ± 120 μg m^{-3} for the three-year sampling period. Averaged TSP mass concentrations were at the similar level in Nov. 2009-Oct. 2010 and Nov. 2010-Oct. 2011, but decreased by ~13% in Nov. 2011-Oct. 2012. TSP concentrations of three years all exceeded the 200 μg m^{-3} yearly TSP concentration limit of China's Ambient Air Quality Standards (AAQS)[11].

Mean (± 1σ) concentrations of total carbon (TC_{TSP}), particulate Pb_{TSP} and Hg_{TSP}, and total gaseous Hg (TGM) were 44.9 ± 26.6 μg m^{-3}, 0.33 ± 0.15 μg m^{-3}, 0.64 ± 0.54 ng m^{-3} and 5.66 ± 2.73 ng m^{-3}, respectively. TC_{TSP} accounted for 13.6%, 15.8% and 15.8% of TSP mass in Nov. 2009-Oct. 2010, Nov. 2010-Oct. 2011 and Nov. 2011-Oct. 2012, respectively. Bi-weekly variation of TC_{TSP} concentrations was consistent with TSP time series.

Hg_{TSP} and TGM concentrations varied significantly, ranging from 0.09 to 2.58 ng m^{-3} for Hg_{TSP} and 1.7 to 10.2 ng m^{-3} for TGM. The annual Hg_{TSP} concentrations were 0.41 ± 0.20 ng m^{-3} (1σ, n=22), 0.80 ± 0.54 ng m^{-3} (1σ, n=25) and 0.69 ± 0.70 ng m^{-3} (1σ, n=22) in Nov. 2009-Oct. 2010, Nov. 2010-Oct. 2011 and Nov. 2011-Oct. 2012, respectively. Minimum and maximum Hg_{TSP} values were all observed in 2012. Hg_{TSP} concentrations in Chinese urban air are generally elevated in a range from 0.11 to 1.18 ng m^{-3} [12]. TGM concentrations reported for urban and industrial areas of China were in the range of 2.7-35 ng m^{-3} [12]. Hg_{TSP} normally makes up a significant proportion of urban airborne Hg in China, and during pollution episodes may approach 10%[12]. In this study, the proportion of Hg_{TSP} in total airborne Hg was highest in winter, accounting for 20.4%, followed by spring (12.5%), suggesting severe Hg_{TSP} pollution in winter and spring in Xi'an. Mean TGM levels observed in Xi'an (5.66 ± 2.73 ng m^{-3}) rank at a moderate level compared with other cities in China. For instance, average TGM concentration in Guiyang was 8.4 ± 4.9 ng m^{-3} in 2001-2002[32] and 7.4 ± 4.8 ng m^{-3} in 2008 autumn[33], respectively. The level of TGM in our study was lower than Chongqing[34] (6.7 ± 0.4 ng m^{-3} in 2006-2007) and Guiyang[32, 35]. However, the concentration was higher than that in Shanghai[36] (2.7 ± 1.7 ng m^{-3} in 2009 summer and autumn) and Ningbo[37] (3.8 ± 1.3 ng m^{-3} in 2007-2008 winter). The average Hg_{TSP} concentrations in Guiyang were 0.37 ± 0.68 ng m^{-3} in the latter half of 2009[35] and 1.33 ng m^{-3} in 2008 autumn[33], respectively, which were 42% lower and 142% higher than average Hg_{TSP} in Xi'an (0.64 ± 0.54 ng m^{-3}). The

Hg_{TSP} concentrations from Shanghai in 2004-2006 were 0.33 and 0.56 ng m^{-3} at different sites[38], which were similar to Hg_{TSP} values in this study.

Xi'an air masses contribute to cross-border transport of elevated Hg_{TSP} (and Pb_{TSP}) and TGM levels to the global atmosphere. Regional inter-province transport of Hg and Pb within China is however also important to consider. Xi'an receives dominant northeast (NE) winds from adjacent coal-producing Shanxi province and the coal-consuming Beijing-Tianjin-Hebei region which has mean annual TGM of 10.4 ng m^{-3} and Hg_{TSP} of 0.6 μg m^{-3} [39]. Inter-regional transport of NE Chinese urban-industrial air masses to Xi'an can therefore be a significant source of TGM, but less so for Hg_{TSP} in our three-year time series.

Seasonal concentrations of TSP, TC_{TSP}, Pb_{TSP} and Hg_{TSP} covary, showing maxima in winter and minima in summer (Figure 1 and Table 1). Similar seasonal patterns were observed from year to year. TSP, TC_{TSP} and Pb_{TSP} concentrations in winter were 2.0 to 2.8 times those in summer. Larger, five-fold, seasonal differences were observed for Hg_{TSP}, ranging from 0.22 ± 0.10 ng m^{-3} in summer to 1.10 ± 0.68 ng m^{-3} in winter (means of all 3 years observed). Much higher Hg_{TSP} concentrations in winter were therefore presumably due to a combination of enhanced coal and biomass emissions owing to the demand for domestic heating, unfavorable meteorological conditions (inversions) and enhanced scavenging of Hg emissions on TSP at low temperature (to form Hg_{TSP})[17]. As shown in Table S1, the heating season (e.g. winter, from mid-Nov. to mid-Mar.) was

characterized by lower temperature, wind speed and rainfall compared to the summer period. Low TSP concentrations in summer were due to a deep mixed layer, high air temperature, high wind speed and scavenging of TSP by precipitation, which favored atmospheric convection, dispersion and removal of Hg_{TSP}. This is also reflected in the weak correlations of TSP (r^2 = 0.22), Pb_{TSP} (r^2 = 0.24) and Hg_{TSP} (r^2 = 0.13) with the number of rain events in the bi-weekly sampling period (Figure S2).

Figure S3 shows the correlations of TSP *vs.* Pb_{TSP}, Hg_{TSP} and TC_{TSP}, respectively, and Pb_{TSP} *vs.* Hg_{TSP}. Strong correlations were observed between Pb_{TSP} and TSP (r^2 = 0.66, p<0.0001, Figure S3A) and between TC_{TSP} and TSP (r^2 = 0.71, p<0.0001, Figure S3C), consistent with the suggestions that Pb[4] and TC_{TSP}[40, 41] derive mainly from coal combustion and motor vehicle emissions in Xi'an. The moderate correlation of Hg_{TSP} and TSP (r^2 = 0.46, p<0.0001, Figure S3B) implies that Hg_{TSP} is not exclusively controlled by TSP and its emission sources. Hg_{TSP} also anti-correlates significantly with mean air temperature (r^2 = 0.39, p<0.01) (figure is omitted) reflecting the well-known gas-particle partitioning of GOM to aerosols in cold air with high TSP levels[17].

Previous studies in Xi'an reported fine particulate ($PM_{2.5}$) $Pb_{PM2.5}$ concentrations during autumn and winter of the 2003-2004 and 2006-2009 periods[4, 42]. As $Pb_{PM2.5}$ and Pb_{TSP} are typically not significantly different in Chinese environments[43, 44], we compare $Pb_{PM2.5}$ and Pb_{TSP} results in Figure 2 for the period 2003-2012 on a bi-weekly basis. A significant (r^2 of 0.31) decline in winter (Dec.-Feb.) mean aerosol Pb, by 4.6% per year,

is observed over the period 2003-2012. Regressing $Pb_{PM2.5}$ only gives the same result from 2003-2012 (r^2 = 0.28) (Figure S4). We examined if the decline was confounded by meteorology, since seasonal Pb_{TSP} is partly controlled by rainfall (Figure S5), and Pb emissions could be related to winter temperature. However, mean bi-weekly temperature and rainfall in Xi'an did not show a trend over 2003-2012, and winter Pb_{TSP} was not correlated with temperature nor with rainfall[45] (Figure S5 and Table S2). We therefore conclude that the progressive decline in Xi'an aerosol Pb reflects a decline in urban-industrial Pb emissions. The large increase in Xi'an industrial coal consumption over the 2003-2012 period (from 3.3 to 7.5 Tg y^{-1}) (Table S3) suggests that emission control technologies, in particular flue gas desulfurization[46], have been efficient in lowering Pb and other heavy metal emissions. Even though Pb_{TSP} concentrations have declined in Xi'an over the past decade, the high exposure levels and potential health implications are still a cause for concern. Despite the decline, wintertime Pb_{TSP} concentrations were repeatedly above China's AAQS[11] of 0.5 μg m^{-3}, while nearly all Pb_{TSP} observations exceeded the US EPA guideline of 0.15 μg m^{-3}. Atmospheric Pb levels in Xi'an should therefore pose a serious health concern.

Pb isotopes Pb isotope ratios can provide complementary information on the sources of Pb. But Pb isotope source tracing in China is complicated due to the wide range of Pb isotope ratios in Pb and other heavy metal ores, as well as in Chinese coal[3]. In this study, Pb_{TSP} isotope ratios ranged from 1.149 to 1.164 for $^{206}Pb/^{207}Pb$ (average of

1.157 ± 0.003) and from 2.103 to 2.133 for $^{208}Pb/^{206}Pb$ (average of 2.120 ± 0.006), respectively (Figure 3 and Table 1). Seasonal variations in $^{208}Pb/^{206}Pb$ or $^{206}Pb/^{207}Pb$ were absent. Figure 3 shows Chinese coal has wide variations in Pb isotopic ratios[47]. $^{206}Pb/^{207}Pb$ ratios for Northern Chinese coal approximately ranged from 1.15 to 1.22 (black squares in Figure 3), with an average of 1.181[48]. Coal combustion samples generally showed higher $^{206}Pb/^{207}Pb$ ratios than those of unleaded gasoline vehicle exhaust samples (from 1.11 to 1.15)[49]. Contaminated (road) dust samples in Nanjing (East China, winter 2011) have an average $^{206}Pb/^{207}Pb$ ratio of 1.171 and $^{208}Pb/^{206}Pb$ of 2.105[50]. Pb isotopic ratios for TSP samples in Xi'an were similar to $^{206}Pb/^{207}Pb$ and $^{208}Pb/^{206}Pb$ ratios of coal combustion, but also to Pb ores, unleaded gasoline and contaminated road dust samples, allowing no clear source appointment.

Hg stable isotopes Significant ranges of variation were observed for $\delta^{202}Hg_{TSP}$ (-1.45 to 0.08‰) and $\delta^{202}Hg_{TGM}$ (-0.59 to 1.11‰), while $\Delta^{199}Hg_{TSP}$ (-0.34 to 0.25‰) and $\Delta^{199}Hg_{TGM}$ (-0.10 to 0.07‰) varied much less (Figure 4). Mean $\Delta^{199}Hg_{TGM}$ (0.00 ± 0.04‰, 1σ, n=21) was not significantly different (t-test, p=0.13) from mean $\Delta^{199}Hg_{TSP}$ (-0.02 ± 0.10‰, 1σ, n=67), and both $\Delta^{199}Hg_{TGM}$ and $\Delta^{199}Hg_{TSP}$ did not correlate with seasonality, meteorology, TSP or TC_{TSP}, Pb_{TSP} or each other. $\delta^{202}Hg_{TSP}$ and $\delta^{202}Hg_{TGM}$ in Xi'an were found to be similar to those in other large Asian cities such as Kolkata and Guiyang[51, 52].

$\delta^{202}Hg_{TSP}$ varied seasonally (Figure 1 and Table 1), with mean $\delta^{202}Hg_{TSP}$ significantly

(t-test, p=0.03) higher in the cold season (Oct.-Mar., -0.71 ± 0.30‰, 1σ, n=32) than in the warm season (Apr.-Sept., -0.87 ± 0.29‰, 1σ, n=35). $\delta^{202}Hg_{TSP}$ was also weakly but significantly correlated with temperature (r^2 = 0.12, p<0.01) and with Hg_{TSP} concentrations (r^2 = 0.09, p=0.02), but not with TSP level. Despite substantial intra-annual variation in $\delta^{202}Hg_{TGM}$, there was no correlation with seasonality or temperature. $\delta^{202}Hg_{TGM}$ was correlated with TGM concentration (r^2 = 0.31, p<0.01), suggesting a possible mixing of different emission sources and/or air masses (Figure 5a). In the following, we will discuss the Hg isotope signatures of potential TGM and Hg_{TSP} sources in Xi'an, i.e. the energy and industrial sectors, and Asian background TGM.

Average boundary layer TGM and Hg_{TSP} levels in the Northern Hemisphere (NH), based on observations at 11 AMNet sites are 1.4 ng m^{-3} and 0.005 ng m^{-3} [53]. Long-range transport of Chinese continental air masses to the NH is therefore a variable, i.e. minor to dominant, source of TGM (1.7 to 10.2 ng m^{-3}), and an insignificant source of Hg_{TSP} (0.09 to 2.58 ng m^{-3}) in our three-year time series. Figure 4 summarizes $\delta^{202}Hg_{TGM}$ and $\Delta^{199}Hg_{TGM}$ from the NH rural areas, with site weighted global means of 0.52 ± 0.40‰ (1σ) and -0.17‰ ± 0.08‰ (1σ), respectively[18, 54-57]. Overall Xi'an $\delta^{202}Hg_{TGM}$ was lower (-0.08 ± 0.41‰, 1σ, n=21) and $\Delta^{199}Hg_{TGM}$ higher (0.00 ± 0.04‰, 1σ, n=21) than the NH background. However, two Xi'an summertime samples with low TGM (1.7 and 1.9 ng m^{-3}) that were only moderately impacted by local TGM emissions define similar $\delta^{202}Hg_{TGM}$ and $\Delta^{199}Hg_{TGM}$ as the NH background: 0.76 ± 0.49‰ and -0.06‰ ± 0.05‰

(1σ, n=2), respectively. Xi'an $\Delta^{199}Hg_{TGM}$ is similar to Guiyang $\Delta^{199}Hg_{TGM}$ [52], while Xi'an $\delta^{202}Hg_{TGM}$ is significantly (p<0.0001) heavier than Guiyang $\delta^{202}Hg_{TGM}$ by 0.5‰, a difference that may partly reflect differences in regional coal $\delta^{202}Hg$ (see below). Figure 4 also summarizes published $\delta^{202}Hg_{TSP}$ and $\Delta^{199}Hg_{TSP}$ from urban-industrial environments, and shows similar observations between Guiyang[52] and Xi'an, while Kolkata observations[51] are more variable in $\Delta^{199}Hg_{TSP}$ and carry lighter $\delta^{202}Hg_{TSP}$. This may reflect a larger share of biomass burning TGM emissions in Kolkata which are thought to carry low $\delta^{202}Hg$ derived from vegetation[18]. Urban-industrial TGM isotope signatures lie on a broadly identifiable mixing line between local sources and the NH background (Figure 4). We use a linearized binary isotope mixing diagram to estimate the $\delta^{202}Hg_{TGM\text{-}anthro}$ of average urban-industrial TGM emissions in Xi'an (Figure 5b); extrapolating 1/TGM to 0 yields $\delta^{202}Hg_{TGM\text{-}anthro}$ of -0.44 ± 0.15‰ (1σ). We observe that annual mean Xi'an $\delta^{202}Hg_{TGM}$ (-0.08 ± 0.41‰, σ, n=21) and our estimate of the Xi'an urban-industrial $\delta^{202}Hg_{TGM}$ end-member (-0.44 ± 0.15‰, 1σ) are significantly (Mann-Whitney test, p<0.001) enriched in the heavier isotopes relative to mean Xi'an $\delta^{202}Hg_{TSP}$ (-0.8 ± 0.3‰, 1σ, n=67). In the following we will compare these observations to bottom-up estimates of an anthropogenic Hg isotope emission inventory[58].

Based on energy-industrial statistics for the Xi'an metropolis, Hg emission factors and appropriate abatement factors for China[31, 59] (Table S4) suggests that local Xi'an Hg emissions are dominated by coal consumption (72%) and cement production (25%).

Little information is available on local Hg speciation of Coal Fired Utility Boiler (CFUB) emissions; here we will assume the global estimate of GEM:GOM:Hg_{TSP} = 50:40:10% for CFUB Hg emissions[60] and 100% GEM from the limestone component in cement production. GEM, GOM and Hg_{TSP} levels in typical Chinese urban environments are 6-7 ng m^{-3}, 0.02 ng m^{-3} and 0.25-1.3 ng m^{-3} [33]. This suggests that anthropogenic GOM emissions are rapidly deposited to the local environment and/or partly scavenged onto TSP to become part of the Hg_{TSP} fraction. GOM therefore represents an insignificant atmospheric fraction, and is unlikely to have confounded our $\delta^{202}Hg_{TGM}$ observations. Shaanxi province is the 3rd largest coal producing region in China and imports little coal from other regions[61]. Chinese coal $\delta^{202}Hg$ and $\Delta^{199}Hg$ have been documented in the literature[20, 21, 23, 28]. Shaanxi coal mean $\delta^{202}Hg$ and $\Delta^{199}Hg$ are -0.67 ± 0.14‰ (1σ, n=3) and -0.05 ± 0.02‰ (1σ, n=3). Sun et al.[23] suggested that $\delta^{202}Hg$ (but not $\Delta^{199}Hg$) signatures of GEM, GOM and Hg_{TSP} species in typical CFUB emissions are fractionated relative to feed coal by approximately 1.0, 0.0 and -0.5‰. This would suggest that relative to Shaanxi feed coal with $\delta^{202}Hg$ of -0.67‰, locally emitted GEM, GOM and Hg_{TSP} would have approximate $\delta^{202}Hg$ of 0.3, -0.7 and -1.2‰ (± 0.5, 0.5, 0.6‰, 1σ). Sun et al.[58] also estimated that limestone derived Hg emissions from the cement sector in China have $\delta^{202}Hg$ similar to the average limestone of -1.6 ± 0.6‰. Taking into account the relative amounts of coal and cement sector Hg_{GEM} emissions (0.5×72% and 25%) and their estimated $\delta^{202}Hg_{GEM}$ (0.3 and -1.6‰), local Xi'an anthropogenic GEM emissions

are estimated to have $\delta^{202}Hg_{GEM}$ of -0.2 ± 0.5‰ based on the bottom-up Hg emission inventory. This estimate compares well to our observed Xi'an $\delta^{202}Hg_{TGM}$ of -0.1 ± 0.4‰ and to the binary mixing estimated $\delta^{202}Hg_{TGM\text{-}anthro}$ of -0.4‰. Similarly, local CFUB dominated GOM and Hg_{TSP} emissions are estimated to have associated $\delta^{202}Hg_{GOM}$ of -0.7 ± 0.5‰ and $\delta^{202}Hg_{TSP}$ of -1.2 ± 0.6‰ in the bottom-up emission inventory and compare well to observed Xi'an $\delta^{202}Hg_{TSP}$ of -0.8 ± 0.3‰, 1σ, n=67. As CFUBs, and by analogy other coal consuming industries, do not induce MIF, the observed $\Delta^{199}Hg_{TSP}$ (-0.02‰) and $\Delta^{199}Hg_{TGM}$ (0.00 ‰) also correspond well to Shaanxi feed coal $\Delta^{199}Hg$ (-0.05‰).

Atmospheric pollution is a serious environmental problem in China that affects air quality, climate and human health. Based on correlations between TSP, TC_{TSP}, Pb_{TSP} and Hg_{TSP} concentrations and Pb_{TSP} and Hg_{TSP} isotope signatures, we find that coal consuming industries and domestic coal use dominate atmospheric Pb and Hg. By comparing aerosol Pb observations made at the same location in Xi'an over the 2003-2012 period we find that Pb levels have declined by 4.6% per year on average. Although TSP, Hg_{TSP} and Pb_{TSP} levels are strongly influenced by climatic factors (especially rainfall), the annual decline is not related to changes in temperature or rainfall over 2003-2012. We therefore suggest the decline reflects a decrease in Pb emissions over the same period. While this is encouraging and likely reflects pollution control measures, further reduction in aerosol Pb levels are required to lower neurodevelopmental risk to children. In this study, we provide seasonal estimates of Chinese urban-industrial TGM,

Hg_{TSP} and Pb_{TSP} isotope signatures that can be used in local human exposure studies and in regional and global tracing of Chinese atmospheric outflow.

Supporting Information (SI)

(1) SI1: Detailed information on results and discussion: Table S1-S4 and Figure S1-S5.

(2) SI2: Raw data of manuscript.

Acknowledgements

This work was supported by the Observatoire Midi-Pyrenees BQR research grant to BG, research grant ERC-2010-StG_20091028 from the European Research Council to JES and the Natural Science Foundation of China (NSFC) (Grant No 41503096) to HX. We thank Jerome Chmeleff for expert management of the OMP ICPMS facilities. We also thank three anonymous reviewers for their critical comments that helped improve the manuscript.

References

(1) USEPA, U.S. Environmental Protective Agency: special report on lead pollution. In 2006.

(2) WHO, World Health Organization. Exposure to mercury: A major public health concern. Geneva: WHO, Public Health and Environment. In 2007.

(3) Flegal, A. R.; Gallon, C.; Ganguli, P. M.; Conaway, C. H., All the Lead in China. *Crit. Rev. Environ. Sci. Technol.* **2013,** *43* (17), 1869-1944.

(4) Xu, H. M.; Cao, J. J.; Ho, K. F.; Ding, H.; Han, Y. M.; Wang, G. H.; Chow, J. C.; Watson, J. G.; Khol, S. D.; Qiang, J., Lead concentrations in fine particulate matter after the phasing out of leaded gasoline in

Xi'an, China. *Atmos. Environ.* **2012,** *46* (46), 217-224.

(5) Feng, L.; Zhang, G. L.; Tan, M. G.; Yan, C. H.; Li, X. L.; Li, Y. L.; Yan, L.; Zhang, Y. M.; Shan, Z., Lead in children's blood is mainly caused by coal-fired ash after phasing out of leaded gasoline in Shanghai. *Environ. Sci. Technol.* **2010,** *44* (12), 4760-4765.

(6) USEPA, Environmental Protection Agency Office of Air Quality Planning and Standards Lead Human Exposure and Health Risk Assessments for Selected Case Studies. Research Triangle Park, North Carolina. In 2007.

(7) Li, C.; Wen, T.; Li, Z.; Dickerson, R. R.; Yang, Y.; Zhao, Y.; Wang, Y.; Tsay, S. C., Concentrations and origins of atmospheric lead and other trace species at a rural site in northern China. *J. Geophys. Res. Atmos.* **2010,** *115* (19), 1485-1490.

(8) Qi, Q.; Yang, Y.; Yao, X.; Ding, L.; Wang, W.; Liu, Y.; Chen, Y.; Yang, Z.; Sun, Y.; Yuan, B., Blood lead level of children in the urban areas in China. *Chinese J. Prev. Med.* **2002,** *23* (3), 162-166.

(9) Chen, G. X.; Zeng, G. Z.; Li, J., Correlations of blood lead levels in infant, in maternal blood and in breast milk. *Chinese J. Prev. Med.* **2006,** *40* (3), 189-191.

(10) Men, M.; Guo, B.K., Investigation on the level of blood lead and its influence factors for 0-6 children in Xi'an. *Shaanxi Med. J.* **2013**, *42 (2)*, 226-228. (In Chinese)

(11) GB 3095-2012. Ambient air quality standards in China. In Inspection and Quarantine of the People's Republic of China, 2012.

(12) Fu, X.; Feng, X.; Sommar, J.; Wang, S., A review of studies on atmospheric mercury in China. *Sci. Total Environ.* **2012,** *421-422* (3), 73-81.

(13) Hsu-Kim, H.; Kucharzyk, K. H.; Zhang, T.; Deshusses, M. A., Mechanisms regulating mercury bioavailability for methylating microorganisms in the aquatic environment: a critical review. *Environ. Sci. Technol.* **2013,** *47* (6), 2441-2456.

(14) Hua, Z.; Feng, X. B.; Larssen, T.; Shang, L. H.; Ping, L., Bioaccumulation of methylmercury versus inorganic mercury in rice (Oryza sativa L.) grain. *Environ. Sci. Technol.* **2010,** *44* (12), 4499-4504.

(15) Zhang, H.; Feng, X.; Larssen, T.; Qiu, G.; Vogt, R. D., In inland China, rice, rather than fish, is the major pathway for methylmercury exposure. *Environ. Health Persp.* **2010,** *118* (9), 1183-1188.

(16) Fu, X. W.; Yang, X.; Lang, X. F.; Zhou, J.; Zhang, H.; Yu, B.; Yan, H. Y.; Lin, C. J.; Feng, X. B., Atmospheric wet and litterfall mercury deposition at urban and rural sites in China. *Atmos. Chem. Phys.* **2016**, *16*, 11547-11562.

(17) Amos, H. M.; Jacob, D. J.; Holmes, C. D.; Fisher, J. A.; Wang, Q.; Yantosca, R. M.; Corbitt, E. S.; Galarneau, E.; Rutter, A. P.; Gustin, M. S., Gas-particle partitioning of atmospheric Hg(II) and its effect on global mercury deposition. *Atmos. Chem. Phys.* **2012**, *11 (10)*, 29441-29477.

(18) Enrico, M.; Roux, G. L.; Marusczak, N.; Heimbürger, L. E.; Claustres, A.; Fu, X.; Sun, R.; Sonke, J. E., Atmospheric mercury transfer to peat bogs dominated by gaseous elemental mercury dry deposition. *Environ. Sci. Technol.* **2016**, *50 (5)*, 2405-2412.

(19) Sonke, J. E.; Blum, J. D., Advances in mercury stable isotope biogeochemistry. *Chem. Geol.* **2013,** *336*, 1-4.

(20) Biswas, A.; Blum, J. D.; Bergquist, B. A.; Keeler, G. J.; Xie, Z., Natural mercury isotope variation in coal deposits and organic soils. *Environ. Sci. Technol.* **2008,** *42* (22), 8303-8309.

(21) Yin, R.; Feng, X.; Chen, J., Mercury Stable Isotopic Compositions in Coals from Major Coal Producing Fields in China and Their Geochemical and Environmental Implications. *Environ. Sci. Technol.* **2014,** *48* (10), 5565-5574.

(22) Sun, R.; Sonke, J. E.; Liu, G.; Zheng, L.; Wu, D., Variations in the stable isotope composition of mercury in coal-bearing sequences: Indications for its provenance and geochemical processes. *Int. J. Coal Geol.* **2014,** *133*, 13-23.

(23) Sun, R.; Sonke, J. E.; Heimbürger, L. E.; Belkin, H. E.; Liu, G.; Shome, D.; Cukrowska, E.; Liousse, C.; Pokrovsky, O. S.; Streets, D. G., Mercury stable isotope signatures of world coal deposits and historical coal combustion emissions. *Environ. Sci. Technol.* **2014,** *48* (13), 7660-7668.

(24) Fu, X.; Heimbürger, L. E.; Sonke, J. E., Collection of atmospheric gaseous mercury for stable isotope analysis using iodine- and chlorine-impregnated activated carbon traps. *J. Anal. Atom. Spectrom.* **2014,** *29* (5), 841-852.

(25) Yeghicheyan, D.; Bossy, C.; Coz, M. B. L.; Douchet, C.; Granier, G.; Heimburger, A.; Lacan, F.; Lanzanova, A.; Rousseau, T. C. C.; Seidel, J. L., A compilation of silicon, rare earth element and twenty-one other trace element concentrations in the natural river water reference material SLRS-5 (NRC-CNRC). *Geostand. Geoanal. Re.* **2013,** *37* (4), 449-467.

(26) Nachtegaal, M.; Marcus, M. A.; Sonke, J. E.; Vangronsveld, J.; Livi, K. J. T.; Lelie, D. V. D.; Sparks, D. L., Effects of in situ remediation on the speciation and bioavailability of zinc in a smelter contaminated soil. *Geochim. Cosmochim. Ac.* **2005,** *69* (19), 4649-4664.

(27) De Muynck, D.; Cloquet, C.; Vanhaecke, F., Development of a new method for Pb isotopic analysis of

archaeological artefacts using single-collector ICP-dynamic reaction cell-MS. *J. Anal. At. Spectrom.* **2008**, *23*, 62-71.

(28) Sun, R.; Enrico, M.; Heimbürger, L. E.; Scott, C.; Sonke, J. E., A double-stage tube furnace—acid-trapping protocol for the pre-concentration of mercury from solid samples for isotopic analysis. *Anal. Bioanal. Chem.* **2013,** *405* (21), 6771-6781.

(29) Blum, J. D.; Bergquist, B. A., Reporting of variations in the natural isotopic composition of mercury. *Anal. Bioanal. Chem.* **2007**, *388*, 353-359.

(30) Estrade, N.; Carignan, J.; Sonke, J. E.; Donard, O. F. X., Measuring Hg isotopes in bio-geo-environmental reference materials. *Geostand. Geoanal. Res.* **2009**, *34*, 79-93.

(31) Xi'an Statistical Yearbook. In China Statistics Press: Xi'an Municipal Bureau of Statistics and NBS Survey Office in Xi'an, 2010-2013.

(32) Feng, X.; Shang, L.; Wang, S.; Tang, S.; Zheng, W., Temporal variation of total gaseous mercury in the air of Guiyang, China. *J. Geophys. Res. Atmos.* **2004,** *109* (3), 215-229.

(33) Liu, N.; Qiu, G.; Landis, M. S.; Feng, X.; Fu, X.; Shang, L., Atmospheric mercury species measured in Guiyang, Guizhou province, southwest China. *Atmos. Res.* **2011,** *100* (1), 93-102.

(34) Yang, Y.; Chen, H.; Wang, D., Spatial and temporal distribution of gaseous elemental mercury in Chongqing, China. *Environ. Monit. Assess.* **2008,** *156* (1-4), 479-489.

(35) Fu, X.; Feng, X.; Qiu, G.; Shang, L.; Zhang, H., Speciated atmospheric mercury and its potential source in Guiyang, China. *Atmos. Environ.* **2011,** *45* (25), 4205-4212.

(36) Friedli, H. R.; Arellano, A. F.; Geng, F.; Cai, C.; Pan, L., Measurements of atmospheric mercury in Shanghai during September 2009. *Atmos. Chem. Phys.* **2010,** *11* (8), 3781-3788.

(37) Nguyen, D. L.; Kim, J. Y.; Shim, S. G.; Zhang, X. S., Ground and shipboard measurements of atmospheric gaseous elemental mercury over the Yellow Sea region during 2007–2008. *Atmos. Environ.* **2011,** *45* (1), 253-260.

(38) Xiu, G.; Cai, J.; Zhang, W.; Zhang, D.; Büeler, A.; Lee, S.; Shen, Y.; Xu, L.; Huang, X.; Zhang, P., Speciated mercury in size-fractionated particles in Shanghai ambient air. *Atmos. Environ.* **2009,** *43* (19), 3145-3154.

(39) Fu, X. W.; Zhang, H.; Wang, X.; Yu, B.; Lin, C. J.; Feng, X. B., Observations of atmospheric mercury in China: a critical review. *Atmos. Chem. Phys.* **2015**, *15 (8)*, 11925-11983.

(40) Cao, J. J.; Wu, F.; Chow, J. C.; Lee, S. C., Characterization and source apportionment of atmospheric

organic and elemental carbon during fall and winter of 2003 in Xi'an, China. *Atmos. Chem. Phys.* **2005,** *5* (11), 3127-3137.

(41) Cao, J. J.; Lee, S. C.; Chow, J. C.; Watson, J. G.; Ho, K. F.; Zhang, R. J.; Jin, Z. D.; Shen, Z. X.; Chen, G. C.; Kang, Y. M., Spatial and seasonal distributions of carbonaceous aerosols over China. *J. Geophys. Res. Atmos.* **2007,** *112*, 1-9. doi:10.1029/2006JD008205, D22S11.

(42) Li, Y. Characterization and source apportionment of carbonaceous aerosols over Xi'an atmosphere. Institute of Earth Environment, Chinese Academy of Sciences, 2004.

(43) Xiao, Y. H.; Liu, S. R.; Tong, F. C.; Kuang, Y. W.; Chen, B. F.; Guo, Y. D., Characteristics and Sources of Metals in TSP and $PM_{2.5}$ in an Urban Forest Park at Guangzhou. *Atmosphere* **2014,** *5* (4), 775-787.

(44) Zhang, N.; Cao, J.; Liu, S.; Zhao, Z. Z.; Xu, H.; Xiao, S., Chemical composition and sources of $PM_{2.5}$ and TSP collected at Qinghai Lake during summertime. *Atmos. Res.* **2014,** *138* (3), 213-222.

(45) Xi'an Statistical Yearbook. In China Statistics Press: Xi'an Municipal Bureau of Statistics and NBS Survey Office in Xi'an, 2004-2013.

(46) Giang, A.; Stokes, L. C.; Streets, D. G.; Corbitt, E. S.; Selin, N. E., Impacts of the minamata convention on mercury emissions and global deposition from coal-fired power generation in Asia. *Environ. Sci. Technol.* **2015**, *49 (9)*, 5326-5335.

(47) Mukai, H.; Furuta, N.; Fujii, T.; Ambe, Y.; Sakamoto, K.; Hashimoto, Y., Characterization of sources of lead in the urban air of Asia using ratios of stable lead isotopes. *Environ. Sci. Technol.* **1993,** *27* (7), 1347-1356.

(48) Mukai, H.; Tanaka, A.; Fujii, T.; Zeng, Y.; Hong, Y.; Tang, J.; Guo, S.; Xue, H.; Sun, Z.; Zhou, J., Regional characteristics of sulfur and lead isotope ratios in the atmosphere at several Chinese urban sites. *Environ. Sci. Technol.* **2001,** *35* (6), 1064-1071.

(49) Chen, J.; Tan, M.; Li, Y.; Zhang, Y.; Lu, W.; Tong, Y.; Zhang, G.; Li, Y., A lead isotope record of shanghai atmospheric lead emissions in total suspended particles during the period of phasing out of leaded gasoline. *Atmos. Environ.* **2005,** *39* (7), 1245-1253.

(50) Liu, E.; Yan, T.; Birch, G.; Zhu, Y., Pollution and health risk of potentially toxic metals in urban road dust in Nanjing, a mega-city of China. *Sci. Total Environ.* **2014,** *476-477*, 522-531.

(51) Das, R.; Wang, X.; ·, B. K.; Webster, R. D.; Sikdar, P. K.; Datta, S., Mercury isotopes of atmospheric particle bound mercury for source apportionment study in urban Kolkata, India. *Elementa: Science of the Anthropocene* **2016**, *4*, 1-12. doi: 10.12952/journal.elementa.000098.

(52) Yu, B.; Fu, X.; Yin, R.; Zhang, H.; Wang, X.; Lin, C. J.; Wu, C.; Zhang, Y.; He, N.; Fu, P., Isotopic composition of atmospheric mercury in China: New evidence for source and transformation processes in air and in vegetation. *Environ. Sci. Technol.* **2016,** *50* (17), 9262-9269.

(53) Lan, X.; Talbot, R.; Castro, M.; Perry, K.; Luke, W., Seasonal and diurnal variations of atmospheric mercury across the US determined from AMNet monitoring data. *Atmos. Chem. Phys.* **2012,** *12* (21), 10569-10582.

(54) Gratz, L. E.; Keeler, G. J.; Blum, J. D.; Sherman, L. S., Isotopic composition and fractionation of mercury in Great Lakes precipitation and ambient air. *Environ. Sci. Technol.* **2010,** *44* (20), 7764-7770.

(55) Sherman, L. S.; Blum, J. D.; Johnson, K. P.; Keeler, G. J.; Barres, J. A.; Douglas, T. A., Mass-independent fractionation of mercury isotopes in Arctic snow driven by sunlight. *Nat. Geosci.* **2010,** *3* (3), 173-177.

(56) Demers, J. D.; Blum, J. D.; Zak, D. R., Mercury isotopes in a forested ecosystem: Implications for air surface exchange dynamics and the global mercury cycle. *Global Biogeochem. Cy.* **2013,** *27* (1), 222-238.

(57) Demers, J. D.; Sherman, L. S.; Blum, J. D.; Marsik, F. J.; Dvonch, J. T., Coupling atmospheric mercury isotope ratios and meteorology to identify sources of mercury impacting a coastal urban□ industrial region near Pensacola, Florida, USA. *Global Biogeochem. Cy.* **2015,** *29* (10), 1689-1705.

(58) Sun, R.; Streets, D. G.; Horowitz, H. M.; Amos, H. M.; Liu, G.; Perrot, V.; Toutain, J. P.; Hintelmann, H.; Sunderland, E. M.; Sonke, J. E., Historical (1850-2010) mercury stable isotope inventory from anthropogenic sources to the atmosphere. *Elementa: Science of the Anthropocene* **2016,** *4*, 1-15. doi: 10.12952/journal.elementa.000091.

(59) UNEP, Global Mercury Assessment 2013: Sources, Emissions, Releases and Environmental Transport; UNEP Chemicals Branch Geneva: Switzerland, 2013.

(60) Pacyna, E. G.; Pacyna, J. M., Global emission of mercury from anthropogenic sources in 1995. *Water Air Soil Poll.* **2002**, *137* (1), 149-165.

(61) Zhang, L.; Wang, S.; Meng, Y.; Hao, J., Influence of mercury and chlorine content of coal on mercury emissions from coal-fired power plants in China. *Environ. Sci. Technol.* **2012**, *46* (11), 6385-6392.

(62) Zhu, B. Q.; Chen, Y. W.; Peng, J. H., Lead isotope geochemistry of the urban environment in the Pearl River Delta. *Appl. Geochem.* **2001,** *16* (4), 409-417.

(63) Zheng, J.; Tan, M.; Shibata, Y.; Tanaka, A.; Li, Y.; Zhang, G.; Zhang, Y.; Shan, Z., Characteristics of lead isotope ratios and elemental concentrations in PM_{10} fraction of airborne particulate matter in Shanghai

after the phase-out of leaded gasoline. *Atmos. Environ.* **2004,** *38* (8), 1191-1200.

(64) Tan, M. G.; Zhang, G. L.; Li, X. L.; Zhang, Y. X.; Yue, W. S.; Chen, J. M.; Wang, Y. S.; Li, A. G.; Li, Y.; Zhang, Y. M., Comprehensive study of lead pollution in Shanghai by multiple techniques. *Anal. Chem.* **2006,** *78* (23), 8044-8050.

(65) Lee, C. S. L.; Li, X. D.; Zhang, G.; Li, J.; Ding, A. J.; Wang, T., Heavy metals and Pb isotopic composition of aerosols in urban and suburban areas of Hong Kong and Guangzhou, South China—Evidence of the long-range transport of air contaminants. *Atmos. Environ.* **2007,** *41* (2), 432-447.

(66) Díaz-Somoano, M.; Kylander, M. E.; López-Antón, M. A.; Suárez-Ruiz, I.; Martínez-Tarazona, M. R.; Ferrat, M.; Kober, B.; Weiss, D. J., Stable lead isotope compositions in selected coals from around the world and implications for present day aerosol source tracing. *Environ. Sci. Technol.* **2009,** *43* (4), 1078-1085.

Figure Legends:

Figure 1. Temporal variations of TSP and Pb_{TSP} concentrations (conc., upper panel), particulate and total gaseous Hg concentrations, $^{206}Pb/^{207}Pb$ ratio (middle panel), and particulate and total gaseous Hg isotope values ($\delta^{202}Hg$, $\Delta^{199}Hg$) during the sampling period in Xi'an.

Figure 2. Summary of published aerosol Pb (μg m^{-3}) observations in Xi'an. Data[4, 42] were made on $PM_{2.5}$, whereas this study measured TSP. The ensemble of observations points at a steady decline in winter time aerosol Pb of about 5% per year over the 2003-2012 period ($r^2 = 0.31$).

Figure 3. Scatter plots of isotopic ratios of Pb ($^{208}Pb/^{206}Pb$ and $^{206}Pb/^{207}Pb$) for TSP samples collected from Nov. 2009 to Oct. 2012 in Xi'an and for potential Pb pollution sources[47-50, 62-66] in China. (the Chinese Pb line was drawn using the data for major lead mines in China[48]).

Figure 4. $\delta^{202}Hg$ and $\Delta^{199}Hg$ signatures of TGM (●) and Hg_{TSP} (■) in Xi'an and at other locations (diverse filled symbols). The dark black striped line ($\Delta^{199}Hg = -0.2\times\delta^{202}Hg - 0.1$) represent the mixing line between the Northern Hemisphere (NH) background TGM and recent industrial TGM emissions discussed in the text. Also shown are coal samples (▲) from three Shaanxi coal mines that supply Xi'an domestic and industrial coal use[18, 23, 39, 51, 52, 54-57].

Figure 5. a): $\delta^{202}Hg_{TGM}$ (‰) as a function of TGM concentration (ng m^{-3}) in Xi'an. b): linearized (1/THg) binary isotope mixing diagram between the Northern Hemispheric background TGM (■, 1.4 ng m^{-3}; $\delta^{202}Hg_{TGM}$ of 0.47 ± 0.45‰, 2σ) and local Xi'an urban-industrial TGM emissions, represented by Shaanxi coal (▲, $\delta^{202}Hg_{Shaanxi\ coal}$ of -0.67 ± 0.28‰, 2σ, and assuming no shift in $\delta^{202}Hg$ between coal Hg and emitted TGM).

Table 1. Seasonal statistics (mean ± 1σ) of TSP (μg m^{-3}), TC_{TSP} (μg m^{-3}), Pb_{TSP} (μg m^{-3}), Hg_{TSP} (ng m^{-3}), total gaseous Hg (TGM) (ng m^{-3}), Pb and Hg isotopic ratios in Xi'an during Nov. 2009 to Oct. 2012. Uncertainties of $^{208}Pb/^{206}Pb$ and $^{206}Pb/^{207}Pb$ are 0.09% and 0.07% (1σ) respectively.

	Spring	Summer	Autumn	Winter	All period
TSP	298.0 ± 105.2	186.9 ± 55.2	255.0 ± 77.2	398.5 ± 103.4	298.5 ± 120.3
TC_{TSP}	32.4 ± 9.6	24.7 ± 13.1	43.3 ± 15.5	68.1 ± 29.8	44.9 ± 26.6
Pb_{TSP}	0.25 ± 0.11	0.25 ± 0.09	0.30 ± 0.10	0.49 ± 0.15	0.33 ± 0.15
Hg_{TSP}	0.51 ± 0.21	0.22 ± 0.10	0.55 ± 0.33	1.10 ± 0.68	0.64 ± 0.54
Hg_{TGM}	4.07 ± 2.69	5.51 ± 1.47	8.31 ± 1.34	5.38 ± 3.29	5.66 ± 2.73
$^{208}Pb/^{206}Pb$	2.118 ± 0.006	2.117 ± 0.007	2.121 ± 0.007	2.122 ± 0.004	2.120 ± 0.006
$^{206}Pb/^{207}Pb$	1.157 ± 0.004	1.157 ± 0.004	1.155 ± 0.004	1.157 ± 0.002	1.157 ± 0.003
$\delta^{202}Hg_{TSP}$ (‰)	-0.92 ± 0.21	-0.89 ± 0.36	-0.72 ± 0.16	-0.68 ± 0.35	-0.80 ± 0.30
$\Delta^{199}Hg_{TSP}$ (‰)	-0.02 ± 0.07	-0.03 ± 0.06	0.01 ± 0.10	-0.05 ± 0.13	-0.02 ± 0.10
$\delta^{202}Hg_{TGM}$ (‰)	0.13 ± 0.61	-0.18 ± 0.13	-0.27 ± 0.23	-0.07 ± 0.46	-0.08 ± 0.41
$\Delta^{199}Hg_{TGM}$ (‰)	0.01 ± 0.03	-0.01 ± 0.03	-0.01 ± 0.03	0.00 ± 0.06	0.00 ± 0.04

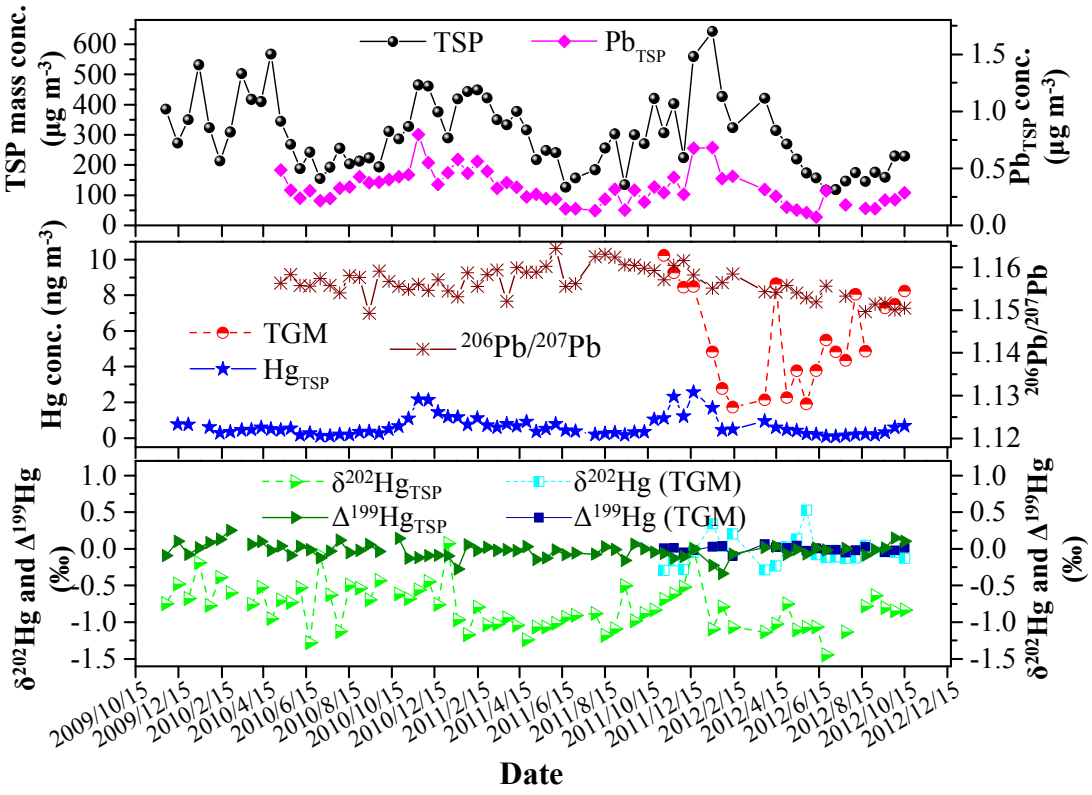
TSP mass conc. (μg m-3)
TSP
PbTSP
PbTSP conc. (μg m-3)
Hg conc. (ng m-3)
TGM
HgTSP
206Pb/207Pb
206Pb/207Pb
δ202HgTSP
Δ199HgTSP
δ202Hg (TGM)
Δ199Hg (TGM)
δ202Hg and Δ199Hg (‰)
Date

Figure 1.

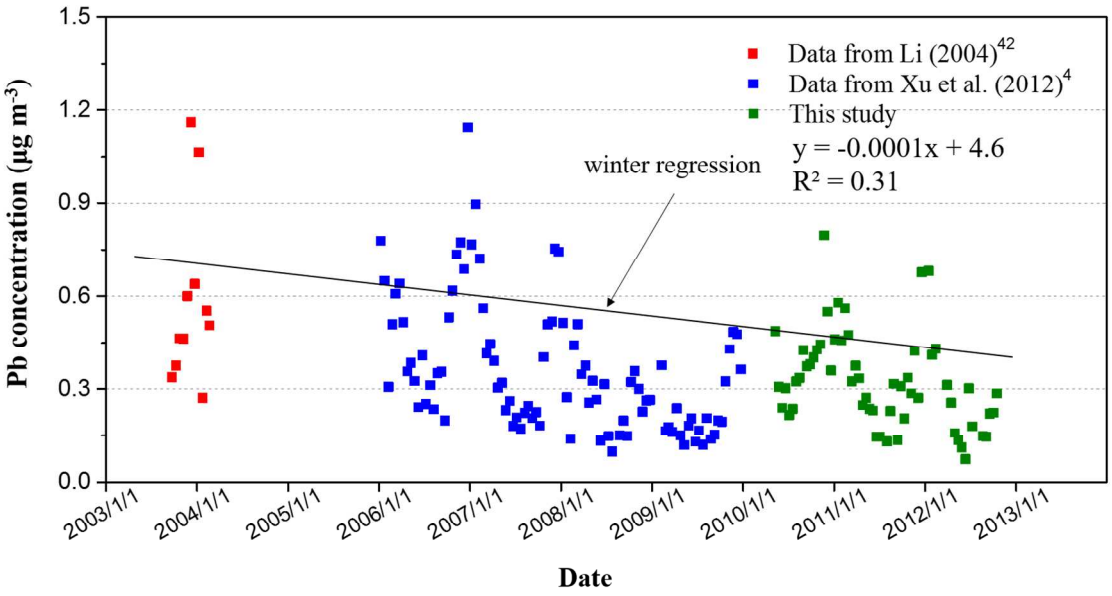
Pb concentration (μg m-3)
1.5
1.2
0.9
0.6
0.3
0.0
2003/1/1
2004/1/1
2005/1/1
2006/1/1
2007/1/1
2008/1/1
2009/1/1
2010/1/1
2011/1/1
2012/1/1
2013/1/1
Date
Data from Li (2004)42
Data from Xu et al. (2012)4
This study
winter regression
y = -0.0001x + 4.6
R² = 0.31

Figure 2.

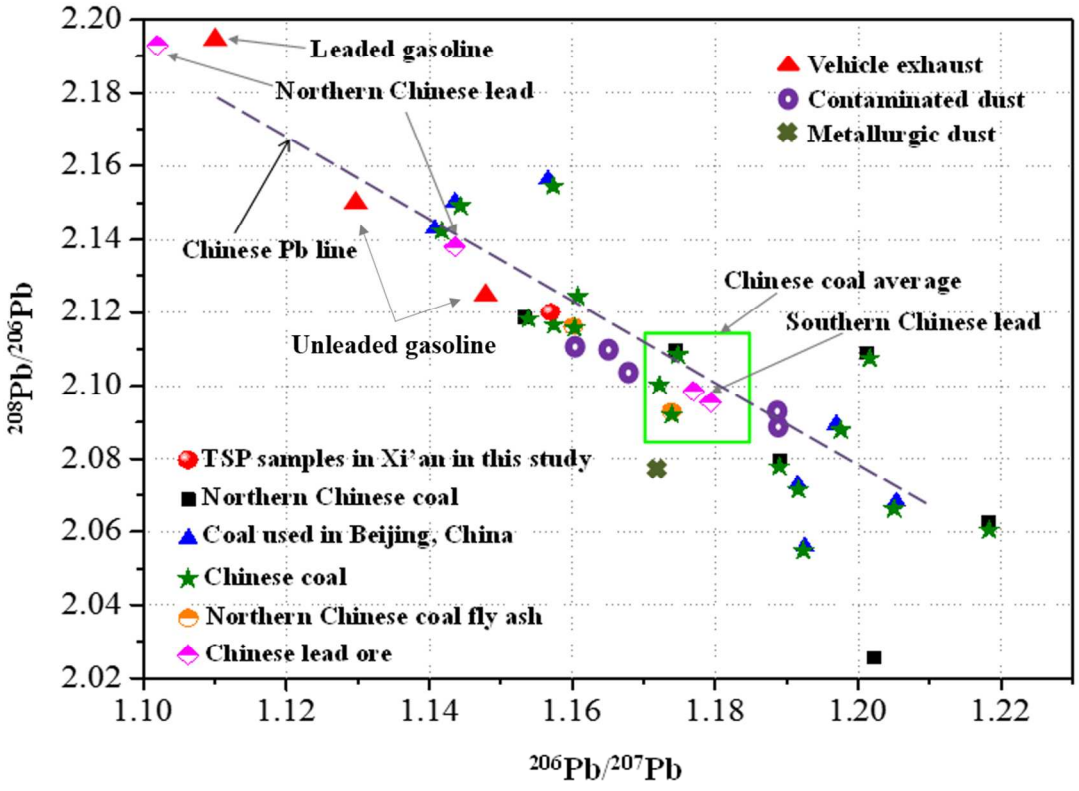
Leaded gasoline
Northern Chinese lead
Chinese Pb line
Unleaded gasoline
Chinese coal average
Southern Chinese lead
Vehicle exhaust
Contaminated dust
Metallurgic dust
TSP samples in Xi'an in this study
Northern Chinese coal
Coal used in Beijing, China
Chinese coal
Northern Chinese coal fly ash
Chinese lead ore
208Pb/206Pb
206Pb/207Pb
2.20
2.18
2.16
2.14
2.12
2.10
2.08
2.06
2.04
2.02
1.10
1.12
1.14
1.16
1.18
1.20
1.22

Figure 3.

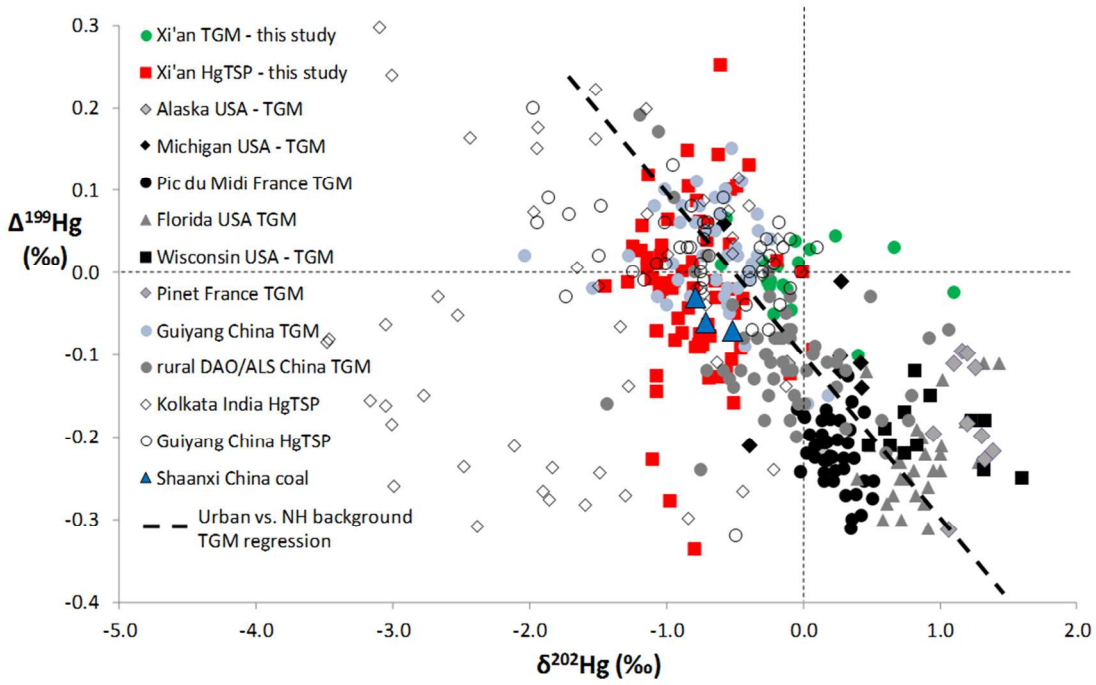
Xi'an TGM - this study
Xi'an HgTSP - this study
Alaska USA - TGM
Michigan USA - TGM
Pic du Midi France TGM
Florida USA TGM
Wisconsin USA - TGM
Pinet France TGM
Guiyang China TGM
rural DAO/ALS China TGM
Kolkata India HgTSP
Guiyang China HgTSP
Shaanxi China coal
Urban vs. NH background TGM regression
Δ199Hg (‰)
δ202Hg (‰)
0.3
0.2
0.1
0.0
-0.1
-0.2
-0.3
-0.4
-5.0
-4.0
-3.0
-2.0
-1.0
0.0
1.0
2.0

Figure 4.

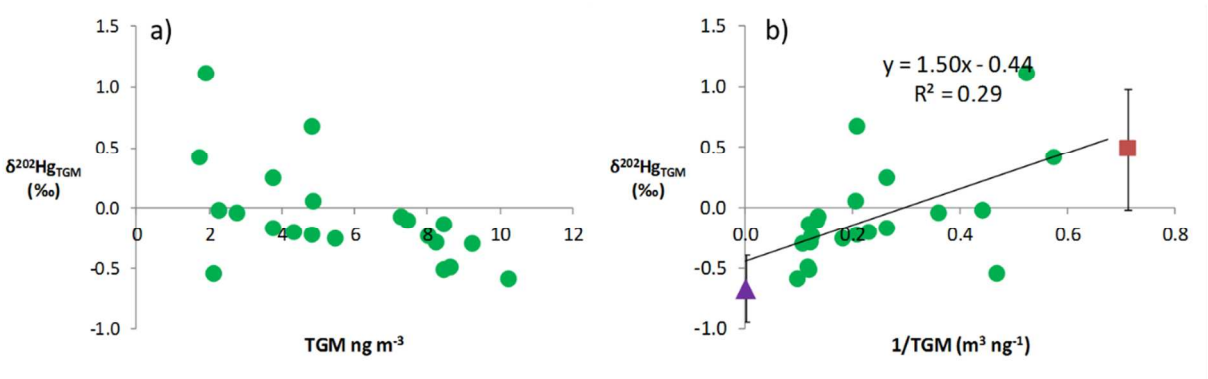
a)
1.5
1.0
0.5
0.0
-0.5
-1.0
δ202HgTGM (‰)
0
2
4
6
8
10
12
TGM ng m-3
b)
y = 1.50x - 0.44
R² = 0.29
0.0
0.2
0.4
0.6
0.8
1/TGM (m3 ng-1)

Figure 5.